

See discussions, stats, and author profiles for this publication at: <https://www.researchgate.net/publication/233998790>

# Control of Crystallinity and Porosity of Covalent Organic Frameworks by Managing Interlayer Interactions Based on Self-Complementary $\pi$ -Electronic Force

ARTICLE in JOURNAL OF THE AMERICAN CHEMICAL SOCIETY · DECEMBER 2012

Impact Factor: 12.11 · DOI: 10.1021/ja3100319 · Source: PubMed

CITATIONS

36

READS

128

## 5 AUTHORS, INCLUDING:



Xiong Chen

Institute for Basic Science

30 PUBLICATIONS 323 CITATIONS

SEE PROFILE



Stephan Irlé

Nagoya University

203 PUBLICATIONS 3,259 CITATIONS

SEE PROFILE



Atsushi Nagai

Institute for Molecular Science

223 PUBLICATIONS 3,919 CITATIONS

SEE PROFILE



Donglin Jiang

Japan Advanced Institute of Science and Tech...

113 PUBLICATIONS 4,899 CITATIONS

SEE PROFILE

# Control of Crystallinity and Porosity of Covalent Organic Frameworks by Managing Interlayer Interactions Based on Self-Complementary $\pi$ -Electronic Force

Xiong Chen,<sup>†</sup> Matthew Addicoat,<sup>‡</sup> Stephan Irle,<sup>‡</sup> Atsushi Nagai,<sup>†</sup> and Donglin Jiang<sup>\*,†,§</sup>

<sup>†</sup>Department of Materials Molecular Science, Institute for Molecular Science, National Institutes of Natural Sciences, 5-1 Higashiyama, Myodaiji, Okazaki 444-8787, Japan

<sup>‡</sup>Department of Chemistry, Graduate School of Science, Nagoya University, Furo-cho, Chikusa-ku, Nagoya 464-8601, Japan

<sup>§</sup>PRESTO, Japan Science and Technology Agency (JST), Chiyoda-ku, Tokyo 102-0075, Japan

## Supporting Information

**ABSTRACT:** Crystallinity and porosity are crucial for crystalline porous covalent organic frameworks (COFs). Here we report synthetic control over the crystallinity and porosity of COFs by managing interlayer interactions based on self-complementary  $\pi$ -electronic forces. Fluoro-substituted and nonsubstituted aromatic units at different molar ratios were integrated into the edge units that stack to trigger self-complementary  $\pi$ -electronic interactions in the COFs. The interactions improve the crystallinity and enhance the porosity by maximizing the total crystal stacking energy and minimizing the unit cell size. Consequently, the COF consisting of equimolar amounts of fluoro-substituted and nonsubstituted units showed the largest effect. These results suggest a new approach to the design of COFs by managing the interlayer interactions.

Porous materials have attracted great attention in many fields of science and technology. Among them, covalent organic frameworks (COFs) are a unique class because they are composed of lightweight elements linked by strong covalent bonds.<sup>1–7</sup> The most intriguing trait is their atomically precise integration of building blocks into periodic two-dimensional (2D) and three-dimensional structures, which endow COFs with high flexibility in the design of skeleton and polygon morphologies.<sup>31</sup> COFs have emerged as predesignable porous materials for gas adsorption<sup>1–7</sup> and provide useful skeletons for the design of a new class of organic semiconductors that feature columnar  $\pi$ -arrays periodically aligned with a nanometer-scale precision.<sup>3,6</sup> In this sense, 2D COFs serve as new platforms for the design of organic 2D materials with structural periodicity that is difficult to achieve with other molecular architectures. However, control over the crystallinity and porosity, which are key parameters in their applications, has been elusive. Here we report the synthetic control of COFs by managing interlayer interactions based on self-complementary  $\pi$ -electronic forces.

We demonstrated the strategy using imine-linked porphyrin COFs in which fluoro-substituted and nonsubstituted arenes at different molar ratios were integrated into the edge units. The porphyrins occupy the vertices and the arene units are located on the edges of mesoporous two-dimensional COFs. Mixtures containing 2,3,5,6-tetrafluoroterephthalaldehyde (TFTA) and

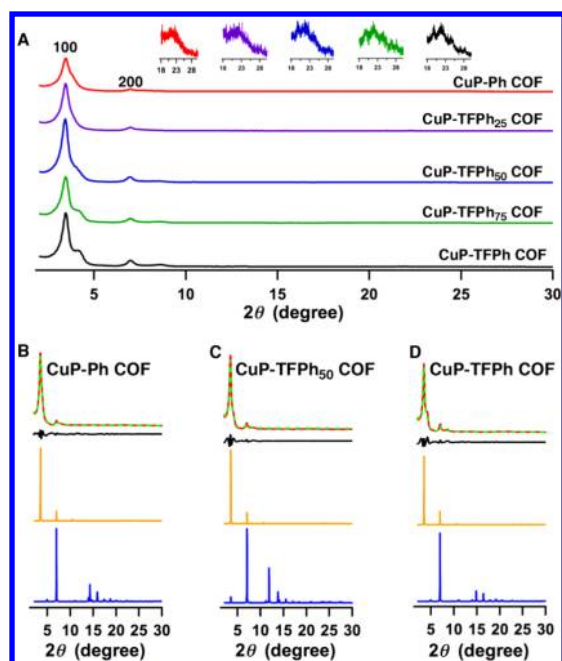
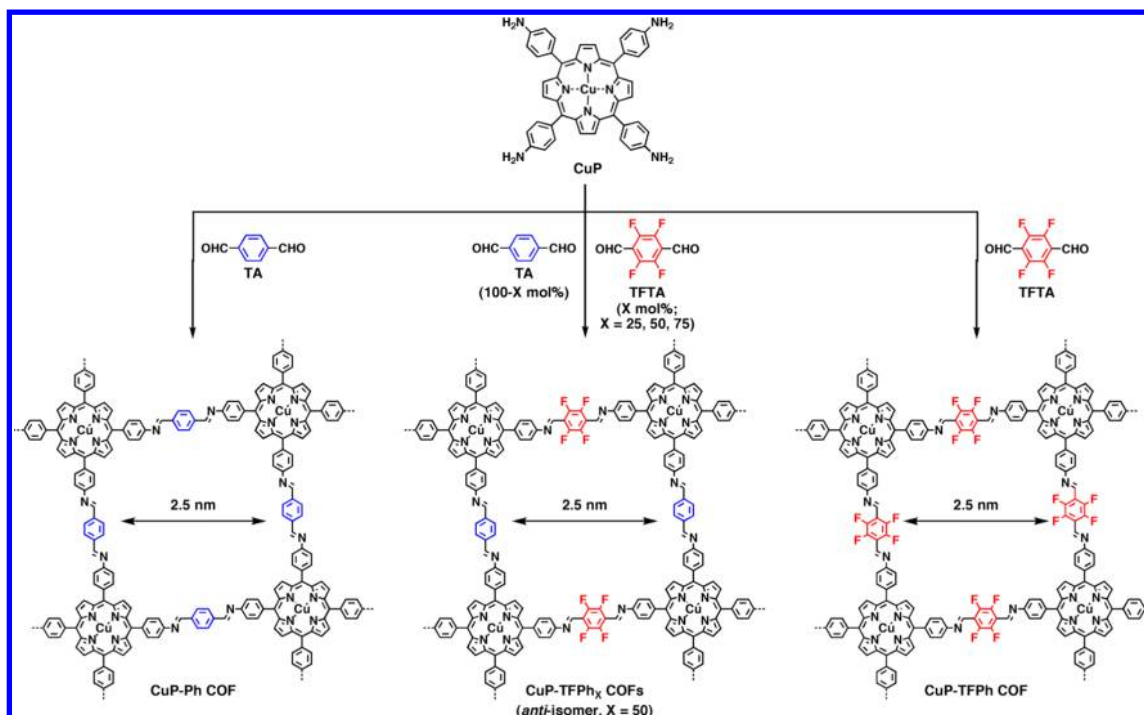
terephthalaldehyde (TA) at different molar ratios were utilized in polycondensation with copper 5,10,15,20-tetrakis(*p*-tetraphenylamino)porphyrin (CuP) under solvothermal conditions, generating five new imine-linked COFs [Chart 1; also see the Supporting Information (SI)]. These reactions exhibited similar isolated yields, indicating that the reactivities of TFTA and TA are similar under the solvothermal conditions. The edge units of the COFs were composed of tetrafluorophenyl (TFPh) and phenyl (Ph) groups at molar ratios of 100/0, 75/25, 50/50, 25/75, and 0/100, respectively. IR spectroscopy, elemental analysis, field-emission scanning electron microscopy, and transmission electron microscopy confirmed the formation of the COFs (Figures S1–S3 and Table S1 in the SI).

Figure 1A shows the X-ray diffraction (XRD) patterns of the five COFs. Each COF exhibited diffraction peaks at 3.4, 6.9, and 20–22°, which were assigned to the (100), (200), and (001) facets, respectively. A significant feature is that the XRD peak intensities were highly dependent on the edge components. For example, the COF bearing only Ph units in the edges (CuP–Ph) exhibited the lowest XRD intensity of ~15000 cps for the (100) facet (red curve). When the content of TFPh units was increased to 25 mol % (CuP–TFPh<sub>25</sub>), the intensity increased to 21000 cps (purple curve). The most explicit increment was observed for CuP–TFPh<sub>50</sub>, which showed an intensity of 30300 cps (blue curve). In this case, the two edge units are present in an equimolar ratio and produce the largest number of self-complementary  $\pi$ -stacked pairs. Consequently, CuP–TFPh<sub>50</sub> shows the strongest self-complementary electronic interactions. Further increments in the TFPh content eventually caused decrements in the XRD intensity (green and black curves). The distinct edge-dependent intensity changes reflect the effective control over the crystallinity of the COF through self-complementary electronic interactions. Such interactions have been employed for the crystal engineering of arene arrays through strengthened  $\pi$ – $\pi$  interactions between fluoro-substituted and nonsubstituted arenes.<sup>8</sup> In the present  $\pi$ -array systems, the enhanced  $\pi$ -interactions improved the crystallinity of the COFs.

Received: October 11, 2012

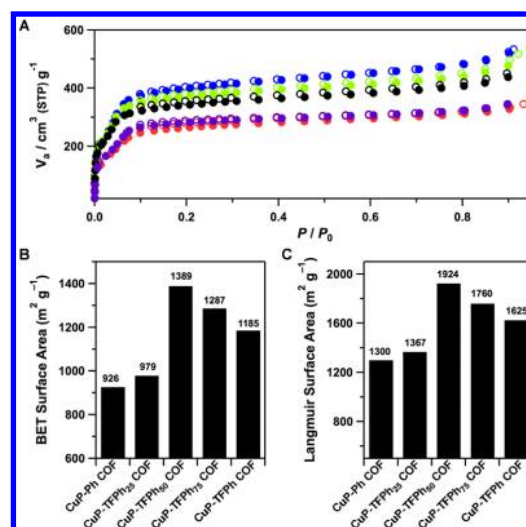
Published: December 27, 2012

Chart 1. Schematic Representation of the Synthesis of COFs Integrated with Self-Complementary  $\pi$ -Electronic Interactions (CuP-TFPh<sub>X</sub>, X = 25, 50, and 75 mol %) and the CuP-Ph and CuP-TFPh Controls



**Figure 1.** (A) XRD patterns of the COFs. The insets show enlarged (001) facets. (B–D) Observed XRD pattern (red), Pawley refinement (green), their difference (black), and simulated patterns using slipped AA stacking (orange) and staggered AB stacking (blue) modes for (B) CuP-Ph, (C) CuP-TFPh<sub>50</sub>, and (D) CuP-TFPh.

Nitrogen sorption isotherm measurements at 77 K were performed to investigate the porosity. All of the COFs exhibited type-IV sorption curves (Figure 2A), indicating the presence of mesopores, in agreement with the theoretical pore sizes. Interestingly, their Brunauer–Emmett–Teller (BET) surface areas were dependent on the edge units, with values of 926, 979, 1389, 1287, and 1185 m<sup>2</sup> g<sup>−1</sup> for CuP-Ph, CuP-



**Figure 2.** (A) Nitrogen sorption isotherm profiles measured at 77 K (red, CuP-Ph COF; purple, CuP-TFPh<sub>25</sub>; blue, CuP-TFPh<sub>50</sub>; green, CuP-TFPh<sub>75</sub>; black, CuP-TFPh). (B) BET and (C) Langmuir surface areas.

TFPh<sub>25</sub>, CuP-TFPh<sub>50</sub>, CuP-TFPh<sub>75</sub>, and CuP-TFPh, respectively (Figure 2B). The largest surface area was observed for CuP-TFPh<sub>50</sub>. The Langmuir surface areas also showed a similar tendency, with CuP-TFPh<sub>50</sub> exhibiting the largest value (1924 m<sup>2</sup> g<sup>−1</sup>; Figure 2C). The pore size distribution profiles revealed the presence of only one type of 2.5 nm wide mesopores in these COFs (Figure S4A–E). The pore volume of the COFs exhibited a maximum of 1.11 cm<sup>3</sup> g<sup>−1</sup> when the TFPh content in the edges was 50 mol %, the same trend as observed for the surface area (Figure S4F). Condensation reactions in other solvents, such as 5:5:1 or 15:5:2 mesitylene/dioxane/6 M AcOH, resulted in series of COFs exhibiting the

same trends in XRD intensity and porosity as those prepared in 5:5:1 (v/v) *o*-dichlorobenzene/BuOH/6 M AcOH (Figures S5 and S6).

The strong correlation between the edge component and the crystallinity and porosity indicates that the self-complementary  $\pi$ -electronic interactions are effective in controlling the crystallinity and porosity of the COFs. To gain insight into the crystalline structure of the COFs, we simulated the XRD patterns using different stacking modes. Pawley refinements yielded XRD curves (Figure 1B–D, dashed green curves) that reproduced the observed patterns (red curves), as evidenced by their negligible differences (black curves), indicating the suitable assignment of the diffraction signals. Simulations with a 0.9 Å slipped AA stacking mode (orange curves) reproduced the XRD signal positions and peak intensities. In sharp contrast, a staggered AB stacking mode (blue curves) could not reproduce the XRD patterns. In the case of the slipped AA stacking mode, the *c* value for CuP–TFPh<sub>50</sub> (3.85 Å) was smaller than those for CuP–Ph and CuP–TFPh (3.97 and 3.98 Å, respectively). The *a* and *b* values for CuP–TFPh<sub>50</sub> (25.2 Å) were also smaller than those for CuP–Ph and CuP–TFPh (25.4 Å). Therefore, CuP–TFPh<sub>50</sub> has a much more compact structure as a result of the strong self-complementary  $\pi$ -stacking interactions. Such a compact unit cell may account for the high porosity.

To evaluate the interlayer interactions quantitatively, we employed the density functional tight binding (DFTB) method including Lennard-Jones (LJ) dispersion (Tables S2 and S3). Table 1 summarizes the total crystal stacking energies per layer

**Table 1. Total Crystal Stacking Energies per Layer ( $E_{\text{stack}}$ ) for the CuP–TFPh<sub>50</sub>, CuP–Ph, and CuP–TFPh COFs**

COF	stacking mode	$E_{\text{stack}}$ (kcal mol <sup>−1</sup> )
<i>anti</i> -CuP–TFPh <sub>50</sub>	0.9 Å slipped AA	68.11
	staggered AB	38.73
<i>syn</i> -CuP–TFPh <sub>50</sub>	1.1 Å slipped AA	64.36
	staggered AB	41.30
CuP–Ph	0.9 Å slipped AA	60.07
	staggered AB	35.34
CuP–TFPh	0.9 Å slipped AA	62.58
	staggered AB	39.28

for different stacking modes. CuP–Ph showed stacking energies of 60.07 and 35.34 kcal mol<sup>−1</sup> for the 0.9 Å slipped AA and staggered AB modes, respectively. On the other hand, the stacking energies for the 0.9 Å slipped AA and staggered AB modes of CuP–TFPh were 62.58 and 39.28 kcal mol<sup>−1</sup>, respectively. In the case of CuP–TFPh<sub>50</sub>, there are two different geometries for the alignment of the TFPh edge units, namely, the *syn* and *anti* isomers. The stacking energies for the *anti* isomers with the 0.9 Å slipped AA and staggered AB modes were 68.11 and 38.73 kcal mol<sup>−1</sup>, respectively, and the *syn* isomers were found to have stacking energies of 64.36 and 41.30 kcal mol<sup>−1</sup>, respectively. Accordingly, the *anti* isomer with the 0.9 Å slipped AA stacking structure is much more stable than the *syn* isomers. These results reveal that the integration of self-complementary  $\pi$ – $\pi$  interactions into the edge units clearly increases the total crystal stacking energy, which gives rise to high crystallinity of the COFs. Figure 3 illustrates the structures of these COFs in the 0.9 Å slipped AA stacking mode.

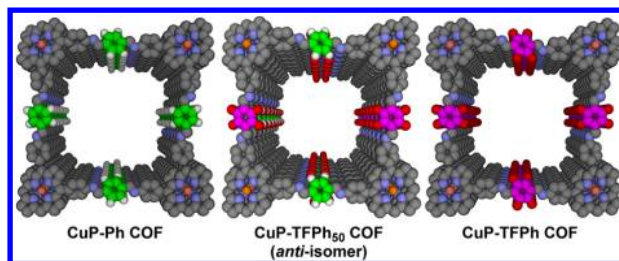


**Figure 3.** The 0.9 Å slipped AA stacking modes of the COFs.

The HOMO and LUMO mapping showed that in CuP–Ph, both the HOMO and LUMO are centered on the CuP units.<sup>9</sup> In contrast, in CuP–TFPh<sub>50</sub>, the HOMO is retained on the CuP units but the LUMO is partially moved to the edge units. This feature is also different from CuP–TFPh, in which the LUMO lies completely on the edge units (Figure S7). Therefore, the edge component strongly affects the distribution of the  $\pi$ -electron clouds in the COFs. The HOMO–LUMO gaps were estimated to be 0.131 and 0.065 eV for CuP–Ph and CuP–TFPh, respectively (Table S2). Remarkably, in CuP–TFPh<sub>50</sub>, the gap was reduced to only 0.05 eV. The decreased HOMO–LUMO gap indicates facilitated electron transfer capability in CuP–TFPh<sub>50</sub>.

In summary, we have demonstrated control of the crystallinity and porosity of COFs by managing self-complementary  $\pi$ -electronic interactions through a comparative study of five newly synthesized COFs. Computational studies in conjunction with structural resolutions revealed that the self-complementary  $\pi$ -electronic force maximizes the total crystal stacking energy and minimizes the unit cell size. As a result, the COFs show improved crystallinity and enhanced porosity, with the greatest effects observed when the interactions are strongest. These interactions also show a prominent effect on changing the  $\pi$ -electron distribution in the framework and lowering the HOMO–LUMO gap. The present work suggests a new means of designing COFs by managing the interlayer interactions.

## ■ ASSOCIATED CONTENT

### Supporting Information

Synthetic details, methods, spectral profiles, microscopic images, computational results, and atomistic coordinates and atomic net charges. This material is available free of charge via the Internet at <http://pubs.acs.org>.

## ■ AUTHOR INFORMATION

### Corresponding Author

jiang@ims.ac.jp

### Notes

The authors declare no competing financial interest.

## ■ ACKNOWLEDGMENTS

We are grateful for the financial support of PRESTO, JST. This work was supported by a Grant-in-Aid for Scientific Research (A) (24245030) from the Ministry of Education, Culture, Sports, Science and Technology, Japan, and partially by the National Natural Science Foundation of China (Grant 21128001).



## ■ REFERENCES

- (1) (a) Côté, A. P.; Benin, A. I.; Ockwig, N. W.; O'Keeffe, M.; Matzger, A. J.; Yaghi, O. M. *Science* **2005**, *310*, 1166. (b) Côté, A. P.; El-Kaderi, H. M.; Furukawa, H.; Hunt, J. R.; Yaghi, O. M. *J. Am. Chem. Soc.* **2007**, *129*, 12914. (c) Han, S. S.; Furukawa, H.; Yaghi, O. M.; Goddard, W. A., III. *J. Am. Chem. Soc.* **2008**, *130*, 11580. (d) Doonan, C. J.; Tranchemontagne, D. J.; Glover, T. G.; Hunt, J. H.; Yaghi, O. M. *Nat. Chem.* **2010**, *2*, 235. (e) Wan, S.; Gandara, F.; Asano, A.; Furukawa, H.; Saeki, A.; Dey, S. K.; Liao, L.; Ambrogio, M. W.; Botros, Y. Y.; Duan, X.; Seki, S.; Stoddart, J. F.; Yaghi, O. M. *Chem. Mater.* **2011**, *23*, 4094.
- (2) (a) Tilford, R. W.; Gemmill, W. R.; zur Loye, H. C.; Lavigne, J. J. *Chem. Mater.* **2006**, *18*, 5296. (b) Tilford, R. W.; Mugavero, S. J., III; Pellechia, P. J.; Lavigne, J. J. *Adv. Mater.* **2008**, *20*, 2741. (c) Lanni, L. M.; Tilford, R. W.; Bharathy, M.; Lavigne, J. J. *J. Am. Chem. Soc.* **2011**, *133*, 13975.
- (3) (a) Wan, S.; Guo, J.; Kim, J.; Ihee, H.; Jiang, D. *Angew. Chem., Int. Ed.* **2008**, *47*, 8826. (b) Wan, S.; Guo, J.; Kim, J.; Ihee, H.; Jiang, D. *Angew. Chem., Int. Ed.* **2009**, *48*, 5439. (c) Ding, X.; Guo, J.; Feng, X.; Honsho, Y.; Guo, J.; Seki, S.; Maitarad, P.; Saeki, A.; Nagase, S.; Jiang, D. *Angew. Chem., Int. Ed.* **2011**, *50*, 1289. (d) Feng, X.; Chen, L.; Dong, Y.; Jiang, D. *Chem. Commun.* **2011**, *47*, 1979. (e) Nagai, A.; Guo, Z.; Feng, X.; Jin, S.; Chen, X.; Ding, X.; Jiang, D. *Nat. Commun.* **2011**, *2*, No. 536. (f) Ding, X.; Chen, L.; Honsho, Y.; Feng, X.; Saengsawang, O.; Guo, J.; Saeki, A.; Seki, S.; Irle, S.; Nagase, S.; Vudhichai, P.; Jiang, D. *J. Am. Chem. Soc.* **2011**, *133*, 14510. (g) Feng, X.; Liu, L.; Honsho, Y.; Saeki, A.; Seki, S.; Irle, S.; Dong, Y.; Nagai, A.; Jiang, D. *Angew. Chem., Int. Ed.* **2012**, *51*, 2618. (h) Feng, X.; Chen, L.; Honsho, Y.; Saengsawang, O.; Liu, L.; Wang, L.; Saeki, A.; Irle, S.; Seki, S.; Dong, Y.; Jiang, D. *Adv. Mater.* **2012**, *24*, 3026. (i) Feng, X.; Ding, X.; Jiang, D. *Chem. Soc. Rev.* **2012**, *41*, 6010. (j) Ding, X.; Feng, X.; Saeki, A.; Seki, S.; Nagai, A.; Jiang, D. *Chem. Commun.* **2012**, *48*, 8952. (k) Feng, X.; Dong, Y.; Jiang, D. *CrystEngComm.* **2012**, DOI: 10.1039/C2CE26371H.
- (4) (a) Kuhn, P.; Antonietti, M.; Thomas, A. *Angew. Chem., Int. Ed.* **2008**, *47*, 3450. (b) Wang, X.; Maeda, K.; Thomas, A.; Takanabe, K.; Xin, G.; Carlsson, J. M.; Domen, K.; Antonietti, M. *Nat. Mater.* **2008**, *8*, 76. (c) Bojdys, M. J.; Jeromenok, J.; Thomas, A.; Antonietti, M. *Adv. Mater.* **2010**, *22*, 2202.
- (5) (a) Campbell, N. L.; Clowes, R.; Ritchie, L. K.; Cooper, A. I. *Chem. Mater.* **2009**, *21*, 204. (b) Hasell, T.; Wu, X.; Jones, J. T. A.; Bacsa, J.; Steiner, A.; Mitra, T.; Trewin, A.; Adams, D. J.; Cooper, A. I. *Nat. Chem.* **2010**, *2*, 750.
- (6) (a) Spitler, E. L.; Dichtel, W. R. *Nat. Chem.* **2010**, *2*, 672. (b) Colson, J. W.; Woll, A. R.; Mukherjee, A.; Levendorf, M. P.; Spitler, E. L.; Shields, V. B.; Spencer, M. G.; Park, J.; Dichtel, W. R. *Science* **2011**, *332*, 228. (c) Spitler, E. L.; Giovino, M. R.; White, S. L.; Dichtel, W. R. *Chem. Sci.* **2011**, *2*, 1588. (d) Spitler, E. L.; Koo, B. T.; Novotney, J. L.; Colson, J. W.; Uribe-Romo, F. J.; Gutierrez, G. D.; Clancy, P.; Dichtel, W. R. *J. Am. Chem. Soc.* **2011**, *133*, 19416. (e) Bunck, D. N.; Dichtel, W. R. *Angew. Chem., Int. Ed.* **2012**, *51*, 1885. (f) Spitler, E. L.; Colson, J. W.; Uribe-Romo, F. J.; Woll, A. R.; Giovino, M. R.; Saldivar, A.; Dichtel, W. R. *Angew. Chem., Int. Ed.* **2012**, *51*, 2623. (g) Koo, B. T.; Dichtel, W. R.; Clancy, P. J. *Mater. Chem.* **2012**, *22*, 17460.
- (7) (a) Patwardhan, S.; Kocherzhenko, A. A.; Grozema, F. C.; Siebbeles, L. D. A. J. *Phys. Chem. C* **2011**, *115*, 11768. (b) Lukose, B.; Kuc, A.; Heine, T. *Chem.—Eur. J.* **2011**, *17*, 2388. (c) Farha, O. K.; Spokoyny, A. M.; Hauser, B. G.; Bae, Y.-S.; Brown, S. E.; Snurr, R. Q.; Mirkin, C. A.; Hupp, J. T. *Chem. Mater.* **2009**, *21*, 3033. (d) Dogru, M.; Sonnauer, A.; Gavryushin, A.; Knochel, P.; Bein, T. *Chem. Commun.* **2011**, *47*, 1707. (e) Ding, S. Y.; Gao, J.; Wang, Q.; Zhang, Y.; Song, W.; Su, C.; Wang, W. J. *J. Am. Chem. Soc.* **2011**, *133*, 19816. (f) Berlanga, I.; Ruiz-González, M. L.; González-Calbet, J. M.; Fierro, J. L. G.; Mas-Ballesté, R.; Zamora, F. *Small* **2011**, *7*, 1207. (g) Berlanga, I.; Mas-Ballesté, R.; Zamora, F. *Chem. Commun.* **2012**, *48*, 7976.
- (8) (a) Dai, C.; Nguyen, P.; Marder, T. B.; Scott, A. J.; Clegg, W.; Viney, C. *Chem. Commun.* **1999**, 2493. (b) Ponzini, F.; Zagha, R.; Hardcastle, K.; Siegel, J. S. *Angew. Chem., Int. Ed.* **2000**, *39*, 2323.
- (c) Collings, J. C.; Roscoe, K. P.; Thomas, R. L.; Batsanov, A. S.; Stimson, L. M.; Howard, J. A. K.; Marder, T. B. *New J. Chem.* **2001**, *25*, 1410. (d) Vangala, V. R.; Nangia, A.; Lynch, V. M. *Chem. Commun.* **2002**, 1304. (e) Gdaniec, M.; Jankowski, W.; Milewska, M. J.; Polonowski, T. *Angew. Chem., Int. Ed.* **2003**, *42*, 3903. (f) Watt, S. W.; Dai, C.; Scott, A. J.; Burke, J. M.; Thomas, R. L.; Collings, J. C.; Viney, C.; Clegg, W.; Marder, T. B. *Angew. Chem., Int. Ed.* **2004**, *43*, 3061. (g) Sundararaman, A.; Zakharov, L. N.; Rheingold, A. L.; Jäkle, F. *Chem. Commun.* **2005**, 1708. (h) Hori, A.; Shinohe, A.; Yamasaki, M.; Nishibori, E.; Aoyagi, S.; Sakata, M. *Angew. Chem., Int. Ed.* **2007**, *46*, 7617. (i) Ni, B.; Wang, C.; Wu, H.; Pei, J.; Ma, Y. *Chem. Commun.* **2010**, *46*, 782. (j) Benitex, Y.; Baranger, A. M. *J. Am. Chem. Soc.* **2011**, *133*, 3687.
- (9) Aradi, B.; Hourahine, B.; Frauenheim, T. *J. Phys. Chem. A* **2007**, *111*, 5678.